drones

MDPI

Article

Mapping Coastal Marine Habitats with RGB and Multispectral UAS Imagery to Support Seaweed Aquaculture Management and Ecosystem Conservation

Isabel Urbina-Barreto [1,2,*,†], Evangelos Alevizos [3,†], Telina Minolalaina Randrianary [4], Manon Museux [5], Ravo A. Mahandrisoa Randriamaroson [5], Anne Chauvin [1], Solofoarisoa Rakotoniaina [4], Sébastien Jan [5], Laurent Barillé [3] and Aline Tribollet [1]

1 LOCEAN-IPSL Laboratory, French National Research Institute for Sustainable Development—IRD, Sorbonne University-IRD-CNRS-MNHN, Parc Technologique Universitaire, 2 Rue Joseph Wetzell, 97490 La Réunion, France
2 ENTROPIE Laboratory, Reunion Island University, 97490 La Réunion, France
3 Institut des Substances et Organismes de la Mer ISOMer, Nantes Université, UR2160, 44000 Nantes, France; evangelos.alevizos@univ-nantes.fr (E.A.); laurent.barille@univ-nantes.fr (L.B.)
4 Geophysics Institute and Observatory of Antananarivo, University of Antananarivo, BP 3843, Antananarivo 101, Madagascar; telina.randrianary@gmail.com (T.M.R.)
5 Nosy Boraha Seaweed Company, Ilot Madame BP04-Ambodifotatra, Sainte-Marie 515, Madagascar; ravo@nosyborahaseaweed.mg (R.A.M.R.); seb@sma.mg (S.J.)
* Correspondence: isabel.urbina-barreto@univ-reunion.fr or isabelurbinab@gmail.com; Tel.: +262-6-92-92-30-47
† These authors contributed equally to this work.

Highlights

What are the main findings?

- RGB and multispectral (MS) UAS imagery, combined with a Random Forest classification model, enabled the distinction between seaweed farms and surrounding benthic habitats and achieved an increased habitat mapping accuracy of 87%, Kappa = 0.82.
- RGB imagery enabled the classification of seaweed cultivation farms (*Kappaphycus alvarezii*), green algal bloom, and sandy bottoms with an accuracy of over 85%. A significant difference was shown between RGB and MS imagery performance (85% vs. 89%). However, RGB imagery alone may provide a satisfactorily accurate and more cost-effective alternative for operational monitoring of shallow habitats under optimal illumination and water clarity conditions.

What are the implications of the main findings?

- This study highlights the central role of visible-spectrum information and supports the use of a cost-effective RGB approach for operational aquaculture monitoring.
- This approach supports integrated marine spatial planning by enabling regular assessment of aquaculture interactions with sensitive coastal marine habitats.

Check for updates

Academic Editor: David R. Green

Received: 1 February 2026
Revised: 2 April 2026
Accepted: 3 April 2026
Published: 10 April 2026

Copyright: © 2026 by the authors. Licensee MDPI, Basel, Switzerland. This article is an open access article distributed under the terms and conditions of the Creative Commons Attribution (CC BY) license.

Abstract

Madagascar's expanding blue economy is largely underpinned by seaweed aquaculture, particularly *Kappaphycus alvarezii* (Cottonii), which offers an alternative to declining small-scale fisheries and strengthens the resilience of coastal socio-ecosystems. Ensuring the sustainability of this economic activity requires effective ecological monitoring of aquaculture sites and surrounding habitats. This study examines and compares the performance of two imaging configurations—an RGB composite derived from a subset of multispectral images capturing red (650 nm), green (560 nm), and blue (450 nm) bands; and a five-band multispectral (MS) image encompassing blue, green, red, red-edge (730 nm),

and near-infrared (840 nm) bands—combined with a Random Forest (RF) classification model, for benthic habitat mapping in a seaweed cultivation context. High-resolution orthomosaics (2 cm/pixel) enabled the discrimination of *Kappaphycus* cultivation plots from three shallow-water habitats: (i) 'benthic macrophytes', which comprise: seagrass meadows and benthic macroalgal; (ii) 'sandy bottom' and (iii) 'green algae'. The RF classification achieved an overall accuracy of 87% (Kappa = 0.82) across ~10 hectares. Producer's accuracy exceeded 80% for *Kappaphycus* cultivation, green algae, and sandy bottom for both the RGB and MS datasets, indicating strong classification performance. However, early-stage seaweed was occasionally misclassified as benthic macrophytes, likely due to its low biomass and weak spectral signature. This UAS-based approach provided a robust and cost-effective framework for monitoring off-bottom seaweed farms and associated natural habitats. This approach supports sustainable aquaculture development and integrated coastal management in Madagascar and comparable tropical reef socio-ecosystems.

Keywords: UAS imagery; seaweed aquaculture; *Kappaphycus alvarezii*; Cottonii; RGB and multispectral imagery; random forest classification model; green algal blooms; benthic habitat mapping; Madagascar

1. Introduction

1.1. Shallow Water Habitat Mapping

Tropical coastal socio-ecosystems represent some of the most ecologically and economically significant environments on Earth. Characterized by high biological diversity and productivity, they encompass a mosaic of interconnected habitats—including seagrass meadows, coral reefs, macroalgal zones, mangroves, intertidal rocky shores, and reef–lagoon complexes. These habitats sustain complex ecological interactions and underpin critical ecosystem services, such as carbon sequestration, shoreline protection, and nursery functions for fish and invertebrates [1,2]. Against this backdrop, the concept of the coastal blue economy has emerged as a globally relevant policy framework, seeking to reconcile marine conservation objectives with sustainable economic development [3]. This framing carries particular weight in low- and middle-income countries such as Madagascar, where coastal communities are highly dependent on marine resources for both food security and livelihood stability [4–6].

Within the spectrum of blue economy activities, seaweed aquaculture has attracted growing attention (e.g., United Nations Global Seaweed Initiative -UNGSI 2025) as a sector capable of delivering ecological co-benefits alongside socioeconomics gains [7,8]. The cultivation of *Kappaphycus alvarezii*, a red algae (Rhodophyta) commercially known as Cottonii (hereinafter referred to as *Kappaphycus*), has undergone rapid expansion in Madagascar over the past 15 years, positioning itself as a viable alternative to declining small-scale (artisanal) fisheries and a source of income diversification in coastal areas. This trajectory is significant insofar as it partially offsets reliance on small-scale capture fisheries—notably, octopus harvesting and subsistence fishing—in shallow reef–lagoon systems [9,10]. However, ensuring the long-term viability of seaweed production necessitates robust monitoring frameworks capable of capturing environmental variability and spatial interactions between aquaculture and co-located natural habitats [11–14].

Advances in geospatial technology and remote sensing imagery—encompassing satellite and UAS-based imagery—provide an increasingly powerful methodological basis for these monitoring requirements in coastal ecosystems [14–16]. Satellite imagery, whilst offering broad spatial coverage and the capacity for long-term monitoring, is constrained by

coarser spatial resolution, atmospheric interference, and inflexible acquisition scheduling. Uncrewed Aerial Systems (UASs, or drones), by contrast, enable the collection of high-resolution imagery at fine spatial and temporal scales, facilitating cost-effective habitat characterization and environmental assessment [17–19]. The integration of RGB (conventional) and multispectral (MS) sensors substantially improves the discriminatory capacity between distinct benthic habitat types and supports the detection of temporal change [20–22]. Recently, Innoncentini et al. (2024) [23] analyzed and recommended four MS indices (ABDI1, ABDI2, CIG, and GNDVI) for the segmentation of images in *Kappaphycus* commercial production. When combined with machine-learning-based image classification, this approach yields detailed, spatially explicit habitat maps with demonstrated utility for spatial planning and aquaculture management [24–26]. UAS-based mapping across visible and near-infrared wavelengths has, in particular, shown strong potential for quantifying seaweed biomass, assessing canopy health, and detecting structural changes in adjacent natural habitats [25,27,28]. However, studies simultaneously assessing both seaweed farming and co-located natural habitats remain scarce. Such a coupled approach is particularly relevant to the holistic perspective needed to support the sustainability of blue economy activities within the preservation of coastal marine socio-ecosystems.

A further application of direct relevance to aquaculture management is the early detection of biological disturbances such as algal blooms, also referred to as "green tides", which can exert adverse effects on both the seaweed aquaculture production system and natural habitats [28,29]. Remote sensing offers an operationally efficient means of identifying such events, thereby enabling timely management intervention, limiting production losses, and supporting ecosystem integrity [29–31]. Despite this potential, systematic remote sensing monitoring remains largely absent from tropical seaweed aquaculture operations, particularly across East Africa seaweed production zones, where farming is conducted predominately in very shallow waters (less than 1 m at low tides) using the off-bottom technique (pegs or lines) anchored to the substrate [9]. Integrating UAS-based approaches into routine monitoring therefore constitutes a strategic priority for advancing both the ecological sustainability and economic resilience of the sector [16,26,32].

1.2. Scope of the Study

This study examines and compares the performance of two imaging configurations: an RGB composite derived from a subset of multispectral images capturing red (650 nm), green (560 nm), and blue (450 nm) bands; and a five-band multispectral (MS) image encompassing blue, green, red, red-edge (730 nm), and near-infrared (840 nm) bands—deployed over the shallow reef–lagoon system of Nosy Boraha (Sainte-Marie Island), Madagascar. The study addresses three interconnected mapping objectives: (i) the delineation of *Kappaphycus* seaweed cultivation sites, (ii) the characterization of co-located shallow-water natural habitats, and (iii) the detection of green algal blooms, with the aim of spatially identifying farms affected by "green tide" episodes. Complementary to these objectives, the study evaluates the spectral discrimination between *Kappaphycus* cultivation and surrounding benthic habitat classes at the seaweed production site, assessing the discriminatory capacity of each sensor configuration for fine-scale habitat mapping in a tropical reef lagoon context. Both datasets (RGB, MS) were integrated within a machine-learning classification workflow to assess their capacity to discriminate cultivated seaweed from key benthic habitat classes—benthic macrophytes, sandy bottom, and green macroalgae—with outputs systematically compared and validated. To our knowledge, this study represents one of the first contributions employing UAS-based multispectral imagery for coastal habitat mapping at a *Kappaphycus* production site in Madagascar.

2. Materials and Methods

2.1. Study Site

Nosy Boraha (also called Sainte-Marie Island) is located on the north-eastern coast of Madagascar. The study was conducted in a ~10 ha (approx. 380 m × 270 m) seaweed farm zone, in the shallow reef system forming a coastal lagoon and located on the N-E side of the island (Figure 1). The lagoon has a mean depth ranging from 1.5 to 3 m, with tidal amplitudes varying between 0.5 and 2 m. Seaweed aquaculture of *Kappaphycus* takes place in the lagoon and is operated by different companies. Nosy Boraha Seaweed company (NBS) has developed such aquaculture in the northern part of the lagoon using the off-bottom lines farming technique, which is typically used in very shallow waters (less than 1 m at low tide) [9]. The total surface area allocated to seaweed farming is estimated at approximately 300 ha, of which cultivation plots occupy only 8.3%, approximately 25 ha (pers. measurements in GIS). Seaweed production areas are primarily located on flat, sandy-bottom areas interspersed with sparse seagrass meadows and benthic macroalgal zones. Seagrass meadows of the genera *Thalassia* spp. and *Halophila* spp. are the most abundant, followed by mixed macroalgal assemblages dominated by *Caulerpa* spp., *Hydroclathrus* spp., and *Acanthopora* spp. (pers. observations).

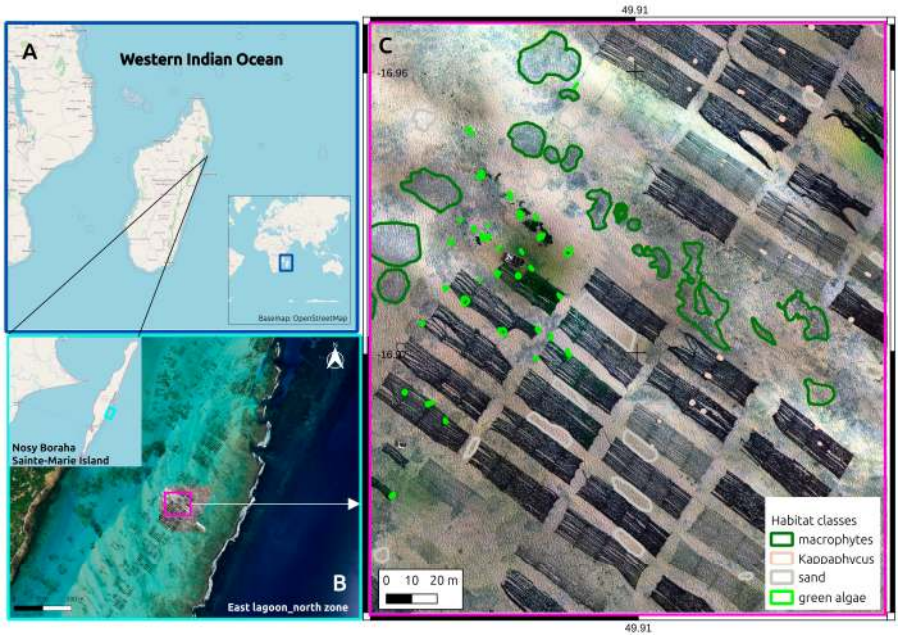


Figure 1. (**A**) Study site location in the Western Indian Ocean: Nosy Boraha, on the north-east coast of Madagascar. (**B**) Google Earth view of northern lagoon of Nosy Boraha with the NBS seaweed farms enlarged (blue frame). (**C**) Ecological zones map, with the RGB composite enlarged, showing a multispectral orthomosaic (pink frame). Four habitat classes were manually annotated: polygons in light brown denoted *Kappaphycus* cultivation; in dark green, benthic macrophytes, comprising mixed assemblages of seagrass meadows (*Halophila* spp.) and benthic macroalgae (*Caulerpa* spp. and *Hydroclathrus* spp.); in light grey, sandy bottoms; and in light green, green macroalgae (*Cladophora* spp.).

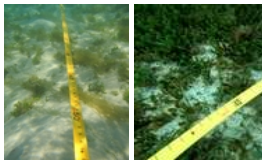
Overall, Nosy Boraha Seaweed company supervises up to 726 cultivation plots managed by 121 farmers. The *Kappaphycus* cultivation cycle, from seeding to harvest, has a mean duration from 35 days to 45 days. Each farmer manages six cultivation plots, which are planted sequentially throughout the month to ensure staggered harvesting and continuous income. This practice results in multiple developmental stages occurring simultaneously within individual farms and across the cultivated area. Farmers are responsible for all stages of the production cycle, including initial planting and routine maintenance, with

cleaning of cultivation lines conducted twice per week. NBS provides technical oversight (five technicians inspecting each plot once per week) by monitoring planting quality, assessing growth performance, detecting signs of parasitism, and determining harvest readiness.

2.2. Field Data Collection

Underwater surveys targeting benthic components and habitat description were conducted by snorkeling in November 2024, following the 'Timed Swims' protocol of Hill and Wilkinson (2004) [33]. The expert swam for approximately 15 min per session, recording observations at 17 fixed GPS points located predominantly on farm structures (fixed points). At each point, a detailed semi-quantitative description of benthic components was noted using abiotic and biotic categories; organisms were identified to genus and species level where possible. For the AUS mapped zone, eight GPS points were selected to ensure representative sampling of *Kappaphycus* farms at different growth stages, while also covering the three habitat classes of interest: benthic macrophytes, sandy bottom, and green algae (Table 1). Underwater images were additionally captured to illustrate benthic components and validate field identifications (Table 1). GPS coordinates were recorded using a SparkFun GNSS RTK Facet receiver (firmware version v3.2), with a positional accuracy of 2.5 m. RTK correction was not applied, as this service was unavailable in the study area.

Table 1. Description of benthic habitat class and visual interpretation on orthomosaic.

Habitat Class			
N°	**Underwater View**	**Visual Interpretation on Orthomosaic**	**Description**
	***Kappaphycus* farms**		
1			*Kappaphycus* farms at different grow stages: Early stage → 1 week after seeding. Mid-stage → 2–3 weeks after seeding. Harvest stage→ 4 weeks to 45 days after seeding.
	Benthic macrophytes		
2			Area dominated by mixed assemblages of benthic macrophytes: seagrass meadows (*Halophila* spp.) and macroalgae (*Caulerpa* spp. and *Hydroclathrus* spp.). Benthic cover >70 %
	Sandy bottom		
3			Unvegetated sand. Benthic cover >90 %
	Green algae		
4			Sampling zones including: *Kappaphycus* farms colonised by green algae and colonised substrate.

2.3. UAS Acquisition and Processing

2.3.1. Overview

The UAS survey was conducted in the early morning of 30 October 2024 (transitional season period), over the shallow intertidal and sub-tidal zones of NBS *Kappaphycus* cultivation. In total, 21 farms corresponding to 126 plots were mapped. At the moment of the survey (7 h), the ebb tide was hide tide (at 6 h 35 min, ~1.5 m depth). The illumination was quite similar during the survey. In the study area, the visibility of water was very good, without any apparent turbidity. The UAS survey had two primary objectives: (i) to acquire very-high-resolution multispectral imagery suitable for the detailed identification and mapping of *Kappaphycus* cultivation plots and associated habitats, including benthic macrophytes such as seagrass meadows, benthic macroalgal assemblages, sandy bottoms, and occurrences of green algal bloom; (ii) to establish an efficient data acquisition and processing workflow enabling reliable spectral discrimination between cultivated seaweed and co-located natural habitats. The overall approach combined in situ underwater census (field data collection), photogrammetric processing, manual annotation (labelling) within a geographic information system (GIS), and the application of machine-learning techniques to discriminate the target classes (Figure 2).

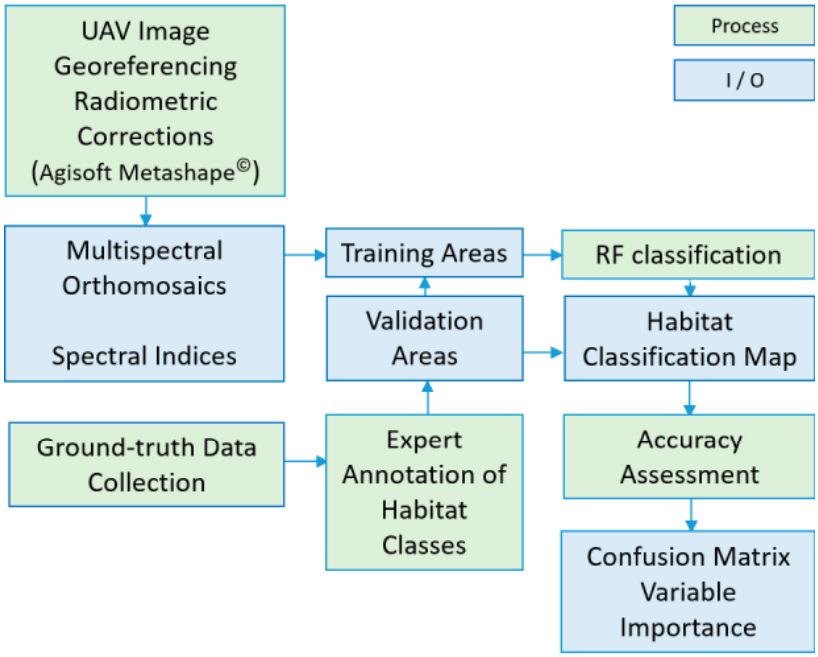


Figure 2. Workflow diagram for collection, processing, and classification of UAS imagery.

2.3.2. UAS Platforms and Sensor Specifications

The DJI Phantom 4 Multispectral (P4M) UAS was employed in this study. This platform integrates a multispectral sensor capturing reflectance data in five narrow spectral bands: blue (450 nm ± 16 nm), green (560 nm ± 16 nm), red (650 nm ± 16 nm), red-edge (730 nm ± 16 nm), and near-infrared (NIR, 840 nm ± 26 nm). The aircraft was equipped with an onboard solar irradiance sensor, which allowed the reflectance calibration of images. The flight's altitude was set to 30 m above the water's surface for achieving optimal ground sampling distance (GSD). Two flights were conducted while applying 70% lateral and frontal overlap, a double grid with a 45° camera angle, and a flight path orientation from away from sun to avoid sun glint and the potential of inducing noise in the images. Gimbal tilt angles and flight orientations relative to the solar azimuth were tested to optimize image sharpness and minimize specular reflection due to sea surface roughness. Off-nadir flights (45°) were preferred over nadir flights (90°) as the former minimize sun glint, particularly

during low solar elevation windows (5 h–7 h local time). Flight tracks were scheduled to enhance overlap geometry and mitigate systematic distortions such as "doming" effects in the Structure-from-Motion (SfM) reconstructions. The visible and red-edge bands are important for detecting contrasting features between seaweed and benthic substrates (sandy bottoms, benthic macrophytes, green algae). The multispectral images were used to compute spectral indices [26], supporting the discrimination of submerged and emergent specimens within the study area.

2.3.3. Image Processing and Photogrammetric Workflow

UAS imagery was processed following a standard photogrammetric workflow using Agisoft Metashape Professional (V2.1). A single global photogrammetric process was conducted, comprising all images from the two surveys. The reconstruction process included image alignment, dense point cloud generation, and orthomosaic production. The following processing parameters were applied: (i) Align photos—medium accuracy; generic preselection: yes; reference preselection "checked": source. (ii) Build dense cloud—quality: medium, filter: mild. (iii) Build DEM—source: dense cloud. (iv) Build orthomosaic—source: DEM. Image reconstruction was performed on a high-performance workstation with a multi-core CPU (central processing unit) and GPU (graphical processor unit) acceleration. Spatial accuracy (ground sampling distance) was enhanced through the use of 8 ground control points (GCPs—GNSS Sarkfun, version v3.2, accuracy of 2.5 m) collected in the field, predominately in fixed reference locations (farm structures). This ensured accurate georeferencing of the orthomosaics. Individual spectral-band orthomosaics were further refined through SfM processing, camera-specific geometric calibration, and the integration of navigation metadata for bundle adjustment and georeferencing, resulting in a final spatial resolution of approximately 2 cm per pixel. The radiometric corrections applied during photogrammetric processing were based on: (a) metadata contained in the image EXIF files, collected by the irradiance sensor (Downwelling Light Sensor) onboard the UAS; and (b) camera exposure parameters. These corrections were implemented within the photogrammetric workflow to improve radiometric consistency across the orthomosaic metadata. A calibration panel was not used on the field for radiometric correction. Consequently, the resulting data correspond to radiometrically normalized reflectance estimates rather than absolute surface reflectance measurements. The water clarity was optimal throughout the survey due to the oligotrophic water conditions in the area; thus, it did not influence the spectral responses of habitats. Though depth ranges from 1.5 to 3 m in the lagoon, the survey took place during low tide resulting in even shallower depths. Under such shallow and optically clear conditions, attenuation and scattering of visible wavelengths within the water column are expected to be minimal, allowing the benthic substrates and vegetation to remain clearly detectable in high-resolution UAS imagery. Therefore, depth-invariant correction methods were not considered, as the depth was shallow enough to utilize the raw spectral responses (Figure 3). The classification included the blue/green and green/red band ratios, which show close affinity with bathymetry [26,34] and can be used as bathymetric proxies for improving spectral information and thus strengthening the predictive capacity of MS data.

The final orthomosaics were imported into QGIS for subsequent analysis and classification. Additional raster layers were generated by computing spectral indices derived from combinations of the multispectral bands. These indices were selected based on the spectral signatures of *Kappaphycus* and shallow-water habitats to enhance spectral separability and improve habitat classification [26] (Figure 3, Table 2). Particularly, in this implementation, the classical NDVI formula was adapted by replacing the NIR band with the red-edge band since the water absorption limited the use of near-infrared wavelengths for benthic habitat

detection. The red-edge band has been suggested by previous studies as a good descriptor of floating aquatic vegetation [25,35]. The index used therefore corresponds more closely to a Red-Edge Normalized Difference Index (NDRE).

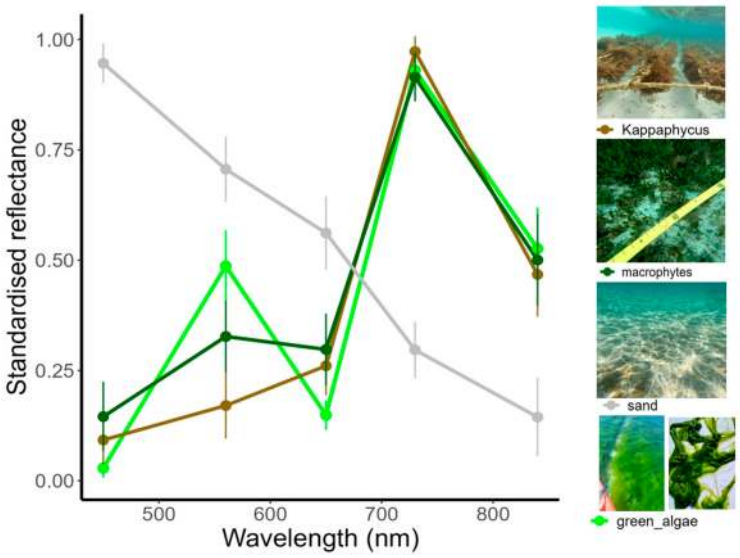


Figure 3. Mean spectral signatures (±95% confidence intervals) of benthic habitat classes: *Kappaphycus* cultivation plots; benthic macrophytes, including mixed assemblages of seagrass and macroalgae; sand and green algae. Spectral signatures were extracted from subsampled homogeneous zones delineated in Figure 1.

Table 2. The image variables used for habitat classification [26]. * The original formula includes the near-infrared (NIR) band; in this implementation, NIR was replaced with the red-edge.

Bands	
450 nm	Blue (B)
530 nm	Green (G)
660 nm	Red (R)
705 nm	Red-edge (RE)
Indices	
$(RE - R)/(RE + R)$	Normalized Difference Red-Edge Index (NDRE)
$(2 \times (G - R - B))/(2 \times (G + R + B))$	Green Leaf Index
$G/(RE + R + G)$	Norm Green *
$R/(RE + R + G)$	Norm Red *
B/G	Blue–green ratio
G/R	Green–red ratio
$(G - R)/(G + R)$	Normalized Difference Green-Red Index (NGRDI)
$[RE - (R - G)]/[RE + (R + G)]$	Red–green NDVI *

2.4. Habitat Discrimination and Training Data

A red–green–blue (RGB) composite orthomosaic was built from MS imagery for visual interpretation of habitat benthic classes. The visual interpretation and labelling on the orthomosaic were carried out by the same expert who conducted the field data collection (underwater observations). Field data, underwater photos, and spatial mapping data were cross-referenced to ensure accurate and consistent labelling of benthic habitat classes.

Four classes were selected for building the training data. Three classes corresponding to habitats: (i) sandy bottom (unvegetated sandy bottoms); (ii) benthic macrophytes, including seagrass meadows (*Halophila* spp.) and macroalgal assemblages (*Caulerpa* spp. and *Hydroclathrus* spp.); and (iii) green algae (*Cladophora* spp.), occurring both within seaweed plots and as patches on the surrounding seabed. The final class corresponded to seaweed farming plots: *Kappaphycus* cultivation, at different cultivation stages, ranging from the first week after seeding to the harvest (Table 1). All habitat polygons were manually delineated in GIS (QGIS-V3.4). Training data are a critical component of the Random Forest classification process and should encompass the full spectral variability of each class [24]. A set of 200 polygons corresponding to the digitized habitat classes were derived from visual interpretation of the RGB composite orthomosaic and subsequently subsampled with 110 polygons assigned for training and 90 for validation (Table 3). These polygons are circles with a radius of four pixels, and they are randomly distributed over the study area with more than three meters' distance between them. From each polygon, a batch of corresponding pixels was extracted (Table 3). The RF model was trained using the corresponding explanatory variables (Table 3), and a 10-fold cross-validation was applied in order to minimize the effect of autocorrelation during the validation stage. The accuracy of the final classification map was evaluated by estimating the confusion matrix and the Kappa coefficient of agreement between the observed (digitized) classes and the RF classification output (Supplementary Materials). In addition, the significance of the differences between the MS and the RGB classifications was evaluated using the McNemars's test [36].

Table 3. The number of polygons and corresponding pixels for the training and validation datasets.

	TRAINING				
	Kappaphycus	**Green algae**	**Macrophytes**	**Sand**	**Total**
nPolygons	31	25	29	25	110
nPixels	706	555	664	565	2490
	VALIDATION				
nPolygons	19	25	21	25	90
nPixels	426	576	480	566	2048

2.5. Random Forest Algorithm

The RF classification algorithm was applied to discriminate *Kappaphycus* cultivation from the sand, benthic macrophyte, and green algae classes. RF was selected due to its high classification accuracy, robustness to over fitting, and availability within commonly used geospatial software [24]. It has been widely and successfully applied in studies of marine vegetation mapping, and specifically for *Kappaphycus* detection [15,24,25,36]. The RF algorithm is based on an ensemble learning approach that combines multiple decision trees constructed from random subsets of the explanatory variables—here, only RGB bands along with MS bands and spectral indices were used—to model the variability of the dependent variable (habitat and *Kappaphycus* classes). RF is a non-parametric ensemble learning method that does not require assumptions about the statistical distribution of predictor variables, which is advantageous when dealing with heterogeneous spectral data derived from multispectral imagery. In our case, the predictor variables included several spectral bands and derived indices that may exhibit strong correlations, especially in the visible range where adjacent bands capture similar reflectance patterns. Random Forest is known to handle such multi-collinearity effectively because each tree is built using a random subset of predictors, reducing the impact of correlated variables.

Another important advantage of RF in remote sensing applications is its ability to capture non-linear relationships between spectral predictors and habitat classes, which are common in benthic environments where reflectance depends not only on substrate type but also on factors such as vegetation density, water depth, and illumination conditions. Furthermore, RF provides embedded estimates of variable importance, which allowed us to identify the spectral bands contributing most to habitat discrimination. Regarding the number of trees, this was based on the number of training data, as has been suggested by [36]. In general, 100–500 trees are recommended for simple RF applications [24]. A 10-fold cross-validation was applied.

In this study, the RF implementation within the EnMap toolbox (QGIS v3.28) was applied, with the following parameters: (i) 100 trees for model training, (ii) subsampling (bootstrap) with replacement, and (iii) using several variables per node, split a number of times equal to the square root of the total variables. Variable importance was assessed by shuffling the values of each variable in each training cycle and measuring the error change in the classification results. The larger the error, the greater the importance of this particular variable, so variables producing larger error increases were considered more influential. Variable importance was evaluated for both multispectral bands and spectral indices.

3. Results

The RF model achieved consistent identification of *Kappaphycus* cultivation within the Nosy Boraha reef lagoon (Figure 4). Sandy bottoms and green algae (*Cladophora* spp.) were identified with high accuracy, whereas the benthic macrophyte class exhibited systematic misclassification. According to the confusion matrix (Table 4), the *Kappaphycus* cultivation, green algae, and sandy bottom habitat classes showed high producer's accuracies (>80%) in both the RGB composite and multispectral datasets, indicating strong classification performance for these classes. The benthic macrophytes class showed the lowest producer's accuracy, reaching 70% when using RGB imagery and increasing to 77% with multispectral data. A recurrent source of error was the misclassification of *Kappaphycus* cultivation as benthic macrophytes (Figure 4B(ii)), leading to an overestimation of the benthic macrophyte class. This misclassification occurred predominantly in plots containing seaweed at early cultivation stages. In addition, sun-glint artefacts, primarily observed over sandy substrates, were occasionally misclassified as either benthic macrophytes or *Kappaphycus* cultivation. It is noteworthy that green algae (*Cladophora* spp.) were reliably detected both as floating material in the water column during plot-cleaning activities (Figure 4B(i)) and when colonizing cultivation plots (Figure 4B(iii)).

Overall, RF classification of the four benthic habitats achieved high accuracies of 85% for RGB imagery and 89% for multispectral imagery (Table 3). Consistently, the Kappa coefficient ranged from 0.80 for RGB data to 0.85 for multispectral data, indicating strong agreement between predicted and observed classes (Table 3).

The overall McNemar test showed that there is a statistically significant difference (p-value = 4.111×10^{-8}) between the MS and RGB classification performances. The number of samples correctly classified only by the MS model exceeded those correctly classified only by the RGB model, indicating the superior performance of the multispectral approach. In particular, when the test was applied per class, it showed that in the case of aquatic vegetation (seaweed, green algae, and macrophytes), the classification based on MS datasets yields statistically more improved predictions than RGB alone (Table 5). In contrast, no significant difference was found for sand, indicating that additional spectral information does not enhance discrimination for this class (Table 5).

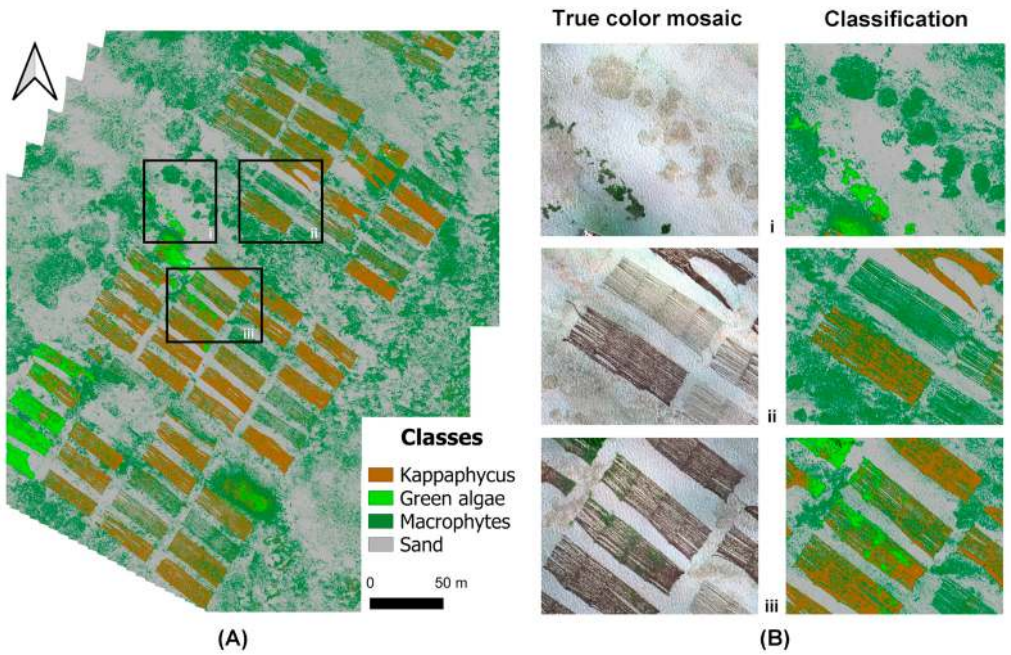


Figure 4. Results for Random Forest classification using the multispectral data and the spectral indices. (**A**) Classification map for the study area (~10 ha); (**B**) close-up panels corresponding to the black rectangles on the main map. Comparison between true-color mosaic and Random Forest classification regarding: (**B**(**i**)) benthic macrophyte patches, sand, and green-algae; (**B**(**ii**)) *Kappaphycus* cultivation plots at early-cultivation and near-harvest stages, with the former being misclassified as benthic macrophytes; (**B**(**iii**)) *Kappaphycus* plots partially covered with green-algae.

Table 4. Confusion matrices and accuracy metrics for 200 validation polygons using: upper: the multispectral (MS) data and the spectral indices; lower: the RGB band subset.

	MULTISPECTRAL Bands + Indices (Cohen's *kappa* = 0.85)					
		OBSERVED				
	User's Acc	**Sand**	**Macrophytes**	**Green Algae**	***Kappaphycus***	
PREDICTED	0.84	0	61	17	**402**	*Kappaphycus*
	0.98	0	10	**513**	1	Green algae
	0.79	45	**380**	46	23	Macrophytes
	0.94	**521**	29	0	0	Sand
	0.89	0.92	0.79	0.89	0.94	Producer's Acc
	RGB Bands (Cohen's *kappa* = 0.80)					
		OBSERVED				
	User's Acc	**Sand**	**Macrophytes**	**Green Algae**	***Kappaphycus***	
PREDICTED	0.82	0	50	32	**363**	*Kappaphycus*
	0.94	0	4	**458**	28	Green algae
	0.7	53	**400**	86	35	Macrophytes
	0.95	**513**	26	0	0	Sand
	0.85	0.91	0.83	0.8	0.85	Producer's Acc

Analysis of variable importance (Figure 5) revealed that the blue band contributed most strongly to class discrimination in the RGB classification. A similar pattern was observed for the multispectral dataset, where the blue band ranked highest, followed by the blue–green ratio and the Green Leaf Index (GLI). These results highlight the importance of blue and blue–green spectral information for distinguishing benthic habitats and cultivated seaweed in shallow coastal environments. Other variables contributed less to the final classification, suggesting a limited additional benefit to enhancing classification accuracy.

Table 5. Results of the McNemar test for evaluating the significance of performance differences regarding individual class outputs and overall classification between the MS and RGB datasets.

McNemar Test per Class			
Winner	**Interpretation**	**Adjusted *p*-Value**	**Class**
MS	Significant	9.72×10^{-5}	*Kappaphycus*
MS	Highly significant	2.55×10^{-13}	Green-algae
MS	Significant	9.30×10^{-3}	Macrophytes
No difference	Not significant	1	Sand
McNemar overall *p*-value = 4.111×10^{-8}			

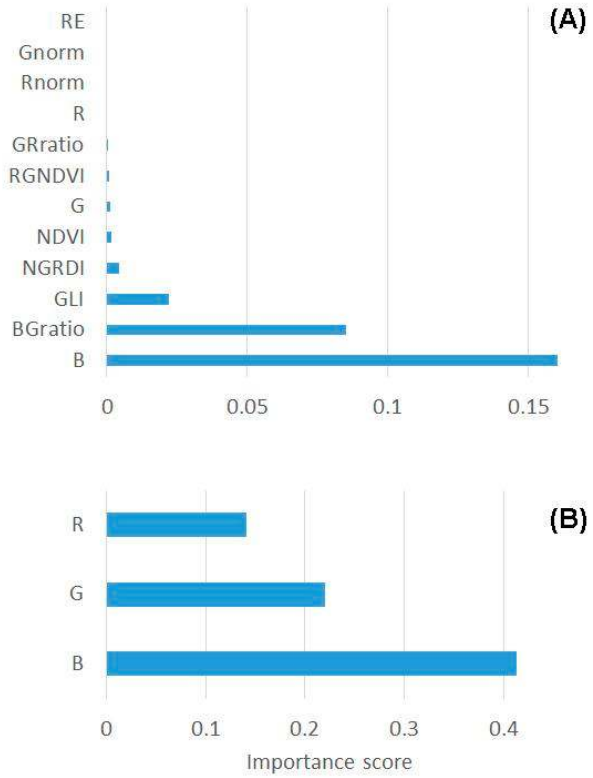


Figure 5. Variable importance scores derived from a 10-fold permutation analysis for the Random Forest classification: (**A**) using multispectral bands and derived spectral indices; and (**B**) using the RGB data. Variables with higher positive scores exert a stronger influence on classification accuracy.

4. Discussion

4.1. Discrimination Capacity of the UAS Approach to Distinguish Farmed Seaweed from Natural Habitats

The strong overall classification performance and high kappa coefficients confirm the robustness and reliability of the RF approach for discriminating benthic habitat classes within the study area by utilizing 55% of ground-truth data for training. Classification results showed that *Kappaphycus* cultivation plots were effectively distinguished from the surrounding natural benthic habitats. They also show the capacity of the approach to discriminate natural habitats dominated by benthic macrophytes from bare sandy bottoms and occurrences of green algal bloom ("green tides"). Both the RGB and MS datasets yielded comparable overall classification accuracies (84% and 89%, respectively), suggesting that the key spectral differences among classes are primarily expressed within the visible part of the electromagnetic spectrum.

The RF model successfully discriminated *Kappaphycus alvarezii*, a rhodophyte, from green algae of the genus *Cladophora* spp., likely owing to their contrasting reflectance patterns in the blue and green spectral bands. In particular, the green algae class achieved consistently high accuracy, due to its strong reflectance in the green spectral region relative to other benthic classes. Our findings are consistent with a previous study by Hamad et al. (2022) in Zanzibar [20]. Our results confirm the value of high-resolution UAS imagery for distinguishing specific habitats dominated by macroalgae and seagrass species based on their pigmentation-related spectral characteristics [21].

The high classification accuracy observed for the sandy bottom class can be attributed to its distinct spectral signature (Figure 3), which contrasts strongly with that of substrates that are colonized or covered by various benthic macrophytes and enhances detectability in shallow-water UAS imagery. Furthermore, our results highlighted that the UAS imagery approach presented limitations in detecting or discriminating accurately the benthic macrophytes class due to a misclassification of *Kappaphycus* during its early cultivation stage. Seaweed seeding of *Kappaphycus* exhibit lower biomass holding lower pigmentation that promotes a weak spectral signature, leading to confusion with the benthic macrophytes class. This misclassification occurred in shallow sandy areas, where a pattern likely driven by spectral mixing between submerged seaweed (approximately 1 m depth) and the underlying sandy substrate produced reflectance values that overlap with those of benthic macrophyte assemblages. Additional errors were observed along the boundaries of *Kappaphycus* cultivation lines, where illumination and edge effects resulted in mixed spectral responses, consistent with previously reported boundary-related artefacts reported in similar contexts [37]. Similar challenges have been reported in previous tropical benthic habitat mapping studies [22,26,38–40]. It has to be noted that in this case study, the improved performance of MS datasets may be attributed to the incorporation of spectral indices using blue and green band combinations such as the blue/green ratio and the GLI, as shown by their importance scores (Table 4). In contrast, the red and red-edge bands appear to contribute considerably less to differentiating aquatic vegetation classes. Though the aquatic vegetation classes appear undifferentiated in the red-edge band (Figure 3), and slightly differentiated in the red band, it is understood that these bands assist in separating aquatic vegetation classes from background sandy bottom effectively. This is due to the absorption of red-edge wavelengths by the upper layer of water (0–50 cm), producing a spectral contrast between submerged sand and floating vegetation. Thus, the off-bottom lines seaweed farming technique presents new challenges for UAS mapping and the spectral distinction of benthic components. Indeed, other studies have recommended more standard vegetation indices (e.g., GNDVI and CIC); however, these were applied to seaweed farming in deeper waters (~20 m) [23]. In our environmental setting—where seaweed farms are co-located with benthic macrophytes—such indices would not provide added value in distinguishing between these classes. In addition, the utility of the red-edge band highlighted by Nurdin et al. (2023) [25] for the detection of *Kappaphycus* plots is valid only when the discrimination takes place between seaweed and background seafloor. In the presented approach, seaweed and benthic macrophytes had overlapping responses in the red-edge, suggesting that the corresponding bands and indices cannot further enhance their separability.

Although multispectral imagery slightly increased overall classification accuracy (89% vs. 85%), this difference is considered statistically significant and substantially increases the ability to detect *Kappaphycus* farms and benthic habitat classes in practice. The difference in accuracy between the RGB and the MS bands may make sense depending on the application. For example, in cases where the accurate quantification of farmed seaweed biomass is important (i.e., aquaculture production management), a multispectral sensor will make a

difference. However, RGB imagery alone may provide a satisfactorily accurate and more cost-effective alternative for operational monitoring of shallow natural benthic habitats under optimal illumination and water clarity conditions (e.g., marine spatial planning/ecosystems conservation management).

4.2. Implications for Marine Spatial Planning and Ecosystem Conservation Management

Accurate mapping of natural habitats co-located with *Kappaphycus* cultivation sites is essential for balancing biodiversity conservation, aquaculture production, and competing coastal uses (e.g., small-scale fisheries and tourism), particularly in ecologically sensitive regions prone to spatial conflicts [12,41,42]. The marine ecosystems of Nosy Boraha, including the Est Lagoon, where extensive seaweed farming occurs, have recently been included in a Terrestrial and Marine Protected Area ("*SORKAY*" TMPA, 2026; source: GRET Sainte-Marie, ONG). The aim of this freshly created TMPA framework is precisely to regulate conflicts of use and protect biodiversity. Improving knowledge of habitat dynamics and health over time will help better support sustainable blue-economy initiatives and terrestrial and marine spatial planning at Nosy Boraha.

Scaling up UAS surveys could thus support marine spatial planning and conservation managers in tracking habitat changes, monitoring seaweed cultivation dynamics, detecting early signs of habitat degradation or recovery (e.g., farm rotation to lead natural habitat rehabilitation), and exploring opportunities to diversify aquaculture practices [12,18,21,43]. Furthermore, high-resolution spatial monitoring should also be adopted for identifying suitable locations for siting future farming activities by assessing substrate suitability and habitat connectivity, and avoiding ecologically vulnerable or heavily impacted areas [4,13,44]. Beyond aquaculture, other economic sectors—particularly tourism, a major economic activity on Sainte-Marie Island—may also benefit from large-scale coastal monitoring to protect beaches and recreational areas. Further research is required to understand the local drivers of the green algal blooms and to develop sustainable mitigation strategies, including, for example, improved wastewater management, infrastructure planning, and outreach education actions.

4.3. Implications for Seaweed Aquaculture Management

Standard RGB imagery alone is sufficient for reliable classification, making it a practical and cost-effective tool for the monitoring of off-bottom seaweed farming zones. RGB imagery enabled accurate detection of *Kappaphycus* cultivation plots, green algal blooms, and bare sandy substrates—three key indicators for seaweed farm management. Under conventional monitoring, each field technician is responsible for approximately 130 cultivation plots per week, requiring in situ inspections to assess growth, culture health, and harvest readiness. These surveys typically require around four hours of daily fieldwork, with technicians covering about 20 ha by paddle, making monitoring both time-consuming and spatially constrained. UAS surveys therefore offer greater scalability, allowing the rapid assessment of large cultivation areas whilst maintaining regular monitoring frequency; our contribution aligns with recent works focusing on this operational scalability [23,29]. These considerations are particularly critical given the rapid dynamics of tropical seaweed farming systems, where algal blooms can develop within a single week. During periods of strong proliferation, emerging problems may remain undetected until the next inspection cycle, leading to delayed responses and biomass losses. Mitigation measures—such as cleaning cultivation lines, removing contaminated lines, restarting cultivation cycles, or temporarily leaving plots fallow—are only effective when implemented early; timely detection is therefore essential for minimizing production losses. This approach can reduce biomass losses and labor requirements, whilst also supporting harvest planning and farm

rotation strategies by identifying spatial variability in growth performance across cultivation plots. Integrating UAS-based assessments in farm management routine could benefit a farm's productivity, reduce losses, and support more sustainable aquaculture practices, as shown in the study by Khan et al. (2024) [45].

4.4. Future Recommendations

UAS monitoring of seaweed aquaculture sites can be limited by environmental and illumination factors, such as specular reflections and water turbidity, which may reduce habitat discrimination accuracy [46]. In this study, a double-grid off-nadir flight configuration was employed to improve SfM reconstruction, resulting in orthomosaics. Nevertheless, accurately discriminating *Kappaphycus* during early cultivation stages remains challenging due to spectral similarities with benthic macrophyte assemblages. Future work could address this limitation through spectral unmixing techniques [47] applied to multispectral or hyperspectral imagery with enhanced radiometric resolution in the visible spectrum. Such approaches are expected to improve early-stage detection of cultivated seaweed and reduce false-positive benthic macrophyte classification. Overall, some limitations should be acknowledged, as they condition the data quality; e.g., the shallow depth range and the optical water quality at the time of acquisition can both greatly influence spectral separability [18,48]. We recommend that future research prioritize the mapping of areas with clearly distinct benthic categories, dominated unambiguously by either seagrass or macroalgae, in order to improve model training.

Regarding the field data collection protocol, it could be further improved by linking and validating the ecological labels assigned on the orthomosaic to georeferenced underwater images corresponding to specific benthic habitat categories. Additionally, future research should seek to distinguish between the organisms constituting the benthic macrophyte class. Where the environmental setting comprises mono-specific zones—dominated by either seagrass or macroalgae, which was not the case in the present study—a finer classification would be both feasible and ecologically meaningful. Finally, the incorporation of additional habitat classes, such as other seagrass genera, would enhance the ecological representativeness and overall robustness of classification in future studies.

Processing large volumes of UAS imagery often requires substantial computational resources. However, combining optimised acquisition and pre-processing workflows with open, cloud-based platforms provides an affordable and scalable solution. These platforms facilitate efficient data processing while supporting data sharing and adherence to FAIR principles, ensuring that cartographic products are findable, accessible, interoperable, and reusable. Implementing such approaches offers tangible benefits for both conservation managers and seaweed producers, enabling high-quality, reproducible monitoring of aquaculture sites and surrounding coastal habitats without prohibitive infrastructure costs.

Finally, regarding green algal bloom events, this study provides a tool for the effective mapping of such occurrences. Scaling up the surface area of the mapped zone, coupled with field observations, could enhance the capacity to determine the origin or triggers of these events, which are likely attributable to a combination of factors, including anthropogenic terrigenous inputs, rainfall, and storm events, as well as seasonal current patterns associated with winter and summer conditions. Furthermore, temporal monitoring through time-series analysis could allow the evolution of these green algal blooms to be tracked over time.

5. Conclusions

The demonstrated effectiveness of both RGB and multispectral UAS imagery underscores their value for the rapid and cost-effective mapping of seaweed aquaculture and

surrounding habitats. Despite the remaining challenges in detecting *Kappaphycus* during early cultivation stages and distinguishing it from benthic macrophyte assemblages, the findings of this study provide a robust methodological foundation for fine-scale habitat mapping and seaweed farm monitoring. Specifically, high-resolution UAS RGB imagery combined with Random Forest classification enables accurate discrimination of cultivated *Kappaphycus* from surrounding benthic habitats in shallow coral reef lagoons. Beyond its technical contributions, this framework offers practical benefits for seaweed aquaculture management, biodiversity conservation, and marine spatial planning—particularly in ecologically sensitive and multi-use coastal systems in low- and-middle income countries such as Madagascar and the Western Indian Ocean region. Overall, our findings corroborate those recently reported by Román et al. (2026) [16] and build upon emerging contributions such as those from Nurdin et al. (2025) [49] and Innocentini et al. (2024) [23] in integrating geospatial technologies and UAS surveys into scalable approaches to support sustainable blue economies and enhance the resilience of tropical coastal socio-ecosystems.

Supplementary Materials: The following supporting information can be downloaded at: https://www.mdpi.com/article/10.3390/drones10040276/s1, Figure S1. Training data and validation results. True color is presented in an RGB orthomosaic (GSD 2 cm/pixel) of the study area, showing the training and validation data points extracted from polygons shown in Figure 1, base map from Google Earth.

Author Contributions: Conceptualization, I.U.-B., E.A., S.J., L.B. and A.T.; methodology, I.U.-B., S.R., T.M.R., R.A.M.R., M.M., S.J., E.A. and L.B.; data collection, I.U.-B., T.M.R., R.A.M.R. and M.M.; data handling, I.U.-B. and E.A.; formal analysis E.A. and L.B.; writing—original draft, I.U.-B. and E.A.; writing—review and editing, I.U.-B., E.A., T.M.R., M.M., L.B., A.C. and A.T.; supervision A.T. and L.B.; co-supervision S.J.; project administration, A.T. and I.U.-B.; funding acquisition, A.T., I.U.-B. and S.J. Photo credits: A.C., T.M.R., M.M. and I.U.-B. All authors have read and agreed to the published version of the manuscript.

Funding: This research was funded by IRD postdoctoral fellowship (2023–2025), Ocean department, project titled: 'RestoEcoDurable', co-supervised by A.T. (LOCEAN, IRD Réunion), Dr Georgeta Stoica (Laboratory ICARE, Réunion-Mayotte), and Dr Victor David (Laboratory IMBE Marseille). The project was supported by the interdisciplinary project 'OA-ME' funded by the Belmont Forum International through the French National Agency ANR (#20-BFOC-0004-01; 2020–2026), an international project coordinated on the French side by A.T. and IRD-LOCEAN laboratory. Nosy Boraha Seaweed company co-supported drone survey funding, provided manpower, and gave logistical means, as well as all information referent to the cultivation plots stages and seaweed aquaculture activity.

Data Availability Statement: The datasets generated during the current study will be made available in an open-access repository on Zenodo.org, DOI: https://doi.org/10.5281/zenodo.18447722, and from the corresponding author upon reasonable request during the study.

Acknowledgments: The authors are very grateful to Nosy Boraha Seaweed company, directed by Sébastien Jan, and all the staff, especially Anthony, JP, Fransicine, Doumé, Jean-Aimé, and Joyce, for their kindness and their involvement in the fieldwork activities, without which this research could not be realized. Special thanks to Kevin CH Andriamanevarivo (Drone Madagascar) and Jerome Mathey (DronoGO) for their help and contribution to the drone flights via advice, conception, assistance, piloting, and aircraft configuration. We are grateful to Michael Y. Roleda for his assistance with macroalgal identification. The authors are thankful to the IRD Madagascar representation: Thierry Portafaix (IRD representative), Regine, Hary, and Hartinulice; and to the IRD Réunion team: Laurence Tibère (IRD representative), Florence, Aurelia, Prisca, and Evelyne, for the overall support and administrative management. We are thankful to La Varangue & CetaMada (Kate), Rando Sainte-Marie (Agostino), and Oclin for logistical support during field campaigns. The authors would like to thank the reviewers for their comments and suggestions, which improved the study and the manuscript.

Conflicts of Interest: Author Manon Museux, Ravo A. Mahandrisoa Randriamaroson and Sébastien Jan were employed by the company Nosy Boraha Seaweed Company. Ambodifotatra–Sainte Marie, Madagascar. The remaining authors declare that the research was conducted in the absence of any commercial or financial relationships that could be construed as a potential conflict of interest.

References

1. Duarte, C.M. The future seagrasses meadows. *Environ. Conserv.* **2002**, *29*, 192–206. [CrossRef]
2. Moberg, F.; Folke, C. Ecological goods and services of coral reef ecosystems. *Ecol. Econ.* **1999**, *29*, 215–233. [CrossRef]
3. OECD. *The Ocean Economy in 2030*; OECD Publishing: Paris, France, 2016. [CrossRef]
4. Valderrama, D.; Cai, J.; Hishamunda, N.; Ridler, N.; Neish, I.C.; Hurtado, A.Q.; Msuya, F.E.; Krishnan, M.; Narayanakumar, R.; Kronen, M.; et al. The Economics of Kappaphycus Seaweed Cultivation in Developing Countries: A Comparative Analysis of Farming Systems. *Aquac. Econ. Manag.* **2015**, *19*, 251–277. [CrossRef]
5. D'agata, S.; Darling, E.S.; Gurney, G.G.; McClanahan, T.R.; Muthiga, N.A.; Rabearisoa, A.; Maina, J.M. Multi-scale determinants of social adaptive capacity in small-scale fishing communities. *Environ. Sci. Policy* **2020**, *108*, 56–66. [CrossRef]
6. Valderrama, D.; Cai, J.; Hishamunda, N.; Ridler, N. *Social and Economic Dimensions of Carrageenan Seaweed Farming in Indonesia*; FAO Fisheries and Aquaculture Technical Paper; Food and Agriculture Organization of the United Nations: Rome, Italy, 2013; Volume 580, p. 217. Available online: https://www.fao.org/4/i3344e/i3344e.pdf (accessed on 15 March 2025).
7. Doumeizel, V.; Aass, K.; McNevin, A.; Cousteau, A.; Yap, A.Y.; Cai, J.; Cottier-Cook, E.; Giercksky, E.; Chen, H.; Skjermo, J. *Seaweed Revolution: A Manifesto for a Sustainable Future*; Lloyd's Register Foundation: London, UK, 2020; pp. 1–16. Available online: https://www.lrfoundation.org.uk/sites/default/files/2024-09/The%20Seaweed%20Manifesto.pdf (accessed on 10 September 2025).
8. Maswati, A.; Suniyyah Puspita, S.; Muis Cahyani, R.A. The Blue Economy as Key to Coastal Development in Small Island Developing States (SIDS). *JWTS—J. World Trade Stud.* **2023**, *8*, 63–70.
9. Msuya, F.E.; Bolton, J.; Pascal, F.; Narrain, K.; Nyonje, B.; Cottier-Cook, E.J. Seaweed farming in Africa: Current status and future potential. *J. Appl. Phycol.* **2022**, *34*, 985–1005. [CrossRef]
10. Jagtap, A.S.; Meena, S.N. Seaweed farming: A perspective of sustainable agriculture and socio-economic development. *Nat. Resour. Conserv. Adv. Sustain.* **2022**, 493–501. [CrossRef]
11. Lyimo, T.; Mvungi, E.; Mgaya, Y. Abundance and diversity of seagrass and macrofauna in the intertidal areas with and without seaweed farming activities in the east coast of Zanzibar. *Tanzan. J. Sci.* **2008**, *34*, 5. [CrossRef]
12. Eggertsen, M.; Halling, C. Knowledge gaps and management recommendations for future paths of sustainable seaweed farming in the Western Indian Ocean. *Ambio* **2021**, *50*, 60–73. [CrossRef]
13. Spillias, S.; Cottrell, R.S.; Kelly, R.; O'Brien, K.R.; Adams, J.; Bellgrove, A.; Kelly, B.; Kilpatrick, C.; Layton, C.; Macleod, C.; et al. Expert perceptions of seaweed farming for sustainable development. *J. Clean. Prod.* **2022**, *368*, 133052. [CrossRef]
14. Bryceson, I. Coastal Aquaculture Developments in Tanzania: Sustainable and Non-sustainable Experiences. *West Indian Ocean J. Mar. Sci.* **2002**, *1*, 1–10.
15. Román, A.; Prasyad, H.; Oiry, S.; Davies, B.F.R.; Brunier, G.; Barillé, L. Mapping intertidal oyster farms using unmanned aerial vehicles (UAV) high-resolution multispectral data. *Estuar. Coast. Shelf Sci.* **2023**, *291*, 108432. [CrossRef]
16. Román, M.; Davies, B.F.R.; Rosa, P.; Oiry, S.; Gernez, P.; Santiago, J.A.; Olabarria, C.; Barillé, L. From pixels to peaks: Integrating LiDAR and RGB drone imagery to map mussel spat on intertidal rocky shores. *Estuar. Coast. Shelf Sci.* **2026**, *329*, 109671. [CrossRef]
17. Anderson, K.; Gaston, K.J. Lightweight unmanned aerial vehicles will revolutionize spatial ecology. *Front. Ecol. Environ.* **2013**, *11*, 138–146. [CrossRef]
18. Nababan, B.; Mastu, L.O.K.; Idris, N.H.; Panjaitan, J.P. Shallow-water benthic habitat mapping using drone with object based image analyses. *Remote Sens.* **2021**, *13*, 4452. [CrossRef]
19. Ventura, D.; Grosso, L.; Pensa, D.; Casoli, E.; Mancini, G.; Valente, T.; Scardi, M.; Rakaj, A. Coastal benthic habitat mapping and monitoring by integrating aerial and water surface low-cost drones. *Front. Mar. Sci.* **2023**, *9*, 1096594. [CrossRef]
20. Hamad, I.Y.; Staehr, P.A.U.; Rasmussen, M.B.; Sheikh, M. Drone-Based Characterization of Seagrass Habitats in the Tropical Waters of Zanzibar. *Remote Sens.* **2022**, *14*, 680. [CrossRef]
21. Oiry, S.; Davies, B.F.R.; Sousa, A.I.; Rosa, P.; Zoffoli, M.L.; Brunier, G.; Gernez, P.; Barillé, L. Discriminating Seagrasses from Green Macroalgae in European Intertidal Areas Using High-Resolution Multispectral Drone Imagery. *Remote Sens.* **2024**, *16*, 4383. [CrossRef]
22. Bajjouk, T.; Mouquet, P.; Ropert, M.; Quod, J.P.; Hoarau, L.; Bigot, L.; Le Dantec, N.; Delacourt, C.; Populus, J. Detection of changes in shallow coral reefs status: Towards a spatial approach using hyperspectral and multispectral data. *Ecol. Indic.* **2019**, *96*, 174–191. [CrossRef]

23. Innocentini, M.M.; Rodrigues, E.F.; Mathion, J.K.; Caritá, E.C.; Simão, L.; Marins, M. Analysis of Multispectral Indices as a Tool for Segmenting and Quantifying the Seaweed Kappaphycus alvarezii in a Commercial Cultivation System. *Biomass* **2024**, *4*, 933–946. [CrossRef]
24. Belgiu, M.; Drăgu, L. Random forest in remote sensing: A review of applications and future directions. *ISPRS J. Photogramm. Remote Sens.* **2016**, *114*, 24–31. [CrossRef]
25. Nurdin, N.; Alevizos, E.; Syamsuddin, R.; Asis, H.; Zainuddin, E.N.; Aris, A.; Oiry, S.; Brunier, G.; Komatsu, T.; Barillé, L. Precision Aquaculture Drone Mapping of the Spatial Distribution of *Kappaphycus alvarezii* Biomass and Carrageenan. *Remote Sens.* **2023**, *15*, 3674. [CrossRef]
26. Alevizos, E.; Nurdin, N.; Aris, A.; Barillé, L. Proximal Sensing for Characterising Seaweed Aquaculture Crop Conditions: Optical Detection of Ice-Ice Disease. *Remote Sens.* **2024**, *16*, 3502. [CrossRef]
27. Borges, D.; Duarte, L.; Costa, I.; Bio, A.; Silva, J.; Sousa-Pinto, I.; Gonçalves, J.A. New Methodology for Intertidal Seaweed Biomass Estimation Using Multispectral Data Obtained with Unoccupied Aerial Vehicles. *Remote Sens.* **2023**, *15*, 3359. [CrossRef]
28. Chen, J.; Li, X.; Wang, K.; Zhang, S.; Li, J. Estimation of Seaweed Biomass Based on Multispectral UAV in the Intertidal Zone of Gouqi Island. *Remote Sens.* **2022**, *14*, 2143. [CrossRef]
29. Joyce, K.E.; Fickas, K.C.; Kalamandeen, M. The unique value proposition for using drones to map coastal ecosystems. *Camb. Prism. Coast. Futures* **2023**, *1*, e6. [CrossRef]
30. Wang, S.; Qin, B. Application of Optical Remote Sensing in Harmful Algal Blooms in Lakes: A Review. *Remote Sens.* **2025**, *17*, 1381. [CrossRef]
31. Xing, Q.; An, D.; Zheng, X.; Wei, Z.; Wang, X.; Li, L.; Tian, L.; Chen, J. Monitoring seaweed aquaculture in the Yellow Sea with multiple sensors for managing the disaster of macroalgal blooms. *Remote Sens. Environ.* **2019**, *231*, 111279. [CrossRef]
32. Elma, E.; Gaulton, R.; Chudley, T.R.; Scott, C.L.; East, H.K.; Westoby, H.; Fitzsimmons, C. Evaluating UAV-based multispectral imagery for mapping an intertidal seagrass environment. *Aquat. Conserv. Mar. Freshw. Ecosyst.* **2024**, *34*, e4230. [CrossRef]
33. Hill, J.; Wilkinson, C. *Methods for Ecological Monitoring of Coral Reefs*; Australian Institute of Marine Science: Townsville, Australia, 2004; Volume 1, p. 117.
34. Roca, M.; Lee, C.B.; Pertiwi, A.P.; Blume, A.; Caballero, I.; Navarro, G.; Traganos, D. Subtidal seagrass and blue carbon mapping at the regional scale: A cloud-native multi-temporal Earth Observation approach. *GISci. Remote Sens.* **2024**, *62*, 2438838. [CrossRef]
35. Cavanaugh, K.C.; Cavanaugh, K.C.; Bell, T.W.; Hockridge, E.G. An Automated Method for Mapping Giant Kelp Canopy Dynamics from UAV. *Front. Environ. Sci.* **2021**, *8*, 587354. [CrossRef]
36. Wicaksono, P.; Aryaguna, P.A.; Lazuardi, W. Benthic habitat mapping model and cross validation using machine-learning classification algorithms. *Remote Sens.* **2019**, *11*, 1279. [CrossRef]
37. Congalton, R.G.; Green, K. *Assessing the Accuracy of Remotely Sensed Data. Principles and Practices*, 3rd ed.; CRC Press: Boca Raton, FL, USA, 2019; p. 346.
38. Vélez-Reyes, M.; Goodman, J.A.; Castrodad-Carrau, A.; Jiménez-Rodriguez, L.O.; Hunt, S.D.; Armstrong, R. Benthic habitat mapping using hyperspectral remote sensing. *Remote Sens. Ocean Sea Ice Large Water Reg.* **2006**, *6360*, 87–97.
39. Casella, E.; Lewin, P.; Ghilardi, M.; Rovere, A.; Bejarano, S. Assessing the relative accuracy of coral heights reconstructed from drones and structure from motion photogrammetry on coral reefs. *Coral Reefs* **2022**, *41*, 869–875. [CrossRef]
40. Oiry, S.; Barillé, L. Using sentinel-2 satellite imagery to develop microphytobenthos-based water quality indices in estuaries. *Ecol. Indic.* **2021**, *121*, 107184. [CrossRef]
41. Chopin, T.; Tacon, A.G.J. Importance of Seaweeds and Extractive Species in Global Aquaculture Production. *Rev. Fish. Sci. Aquac.* **2021**, *29*, 139–148. [CrossRef]
42. Mirera, D.O.; Kimathi, A.; Ngarari, M.M.; Magondu, E.W.; Wainaina, M.; Ototo, A. Societal and environmental impacts of seaweed farming in relation to rural development: The case of Kibuyuni village, south coast, Kenya. *Ocean Coast. Manag.* **2020**, *194*, 105253. [CrossRef]
43. Spillias, S.; von Herzen, B.; Holmgren, D. Marine permaculture: Design principles for productive seascapes. *One Earth* **2024**, *7*, 431–443. [CrossRef]
44. Broch, O.J.; Alver, M.O.; Bekkby, T.; Gundersen, H.; Forbord, S.; Handå, A.; Skjermo, J.; Hancke, K. The kelp cultivation potential in coastal and offshore regions of Norway. *Front. Mar. Sci.* **2019**, *5*, 529. [CrossRef]
45. Khan, N.; Sudhakar, K.; Mamat, R. Macroalgae farming for sustainable future: Navigating opportunities and driving innovation. *Heliyon* **2024**, *10*, e28208. [CrossRef]
46. Doukari, M.; Batsaris, M.; Papakonstantinou, A.; Topouzelis, K. A protocol for Aerial Survey in Coastal Areas Using UAS. *Remote Sens.* **2019**, *11*, 1913. [CrossRef]
47. Uhrin, A.V.; Townsend, P.A. Improved seagrass mapping using linear spectral unmixing of aerial photographs. *Estuar. Coast. Shelf Sci.* **2016**, *171*, 11–22. [CrossRef]

48. Jaud, M.; Geindre, M.; Bertin, S.; Benoît, Y.; Cordier, E.; Flo'c, F.; Augereau, E.; Martins, K. Correction of Refraction Effects on Unmanned Aerial Vehicle Structure-from-Motion Bathymetric Survey for Coral Reef Roughness Characterisation. *Remote Sens.* **2025**, *17*, 3846. [CrossRef]
49. Nurdin, N.; Agus, A.; MAkbar, A.S. Seasonality of *Kappaphycus alvarezii* production trends in South Sulawesi using UAV monitoring. *Remote Sens. Appl. Soc. Environ.* **2025**, *39*, 101659.

Disclaimer/Publisher's Note: The statements, opinions and data contained in all publications are solely those of the individual author(s) and contributor(s) and not of MDPI and/or the editor(s). MDPI and/or the editor(s) disclaim responsibility for any injury to people or property resulting from any ideas, methods, instructions or products referred to in the content.